



Identification and molecular docking of two novel peptides with xanthine oxidase inhibitory activity from *Auxis thazard*

Liuyi WEI¹ , Hongwu JI^{1,2,3,4,5*}, Wenkui SONG¹, Shuo PENG¹, Suhong ZHAN¹, Yushan QU¹, Ming CHEN¹, Di ZHANG¹, Shucheng LIU^{1,2,3,4,5,6}

Abstract

Auxis thazard meat was hydrolyzed by alkaline protease. *Auxis thazard* hydrolysate (ATH) obtained was isolated by ultrafiltration, size exclusion chromatography and reversed-phase high-performance liquid chromatography. Two peptides with high XOD inhibitory activity purified from ATH were identified as Pro-Asp-Leu (PDL, 344.87 Da) and Ser-Val-Gly-Gly-Ala-Leu (SVGGAL, 504.26 Da) by UPLC-MS/MS, which possessed high in vitro XOD inhibitory activity with the IC₅₀ values of 4.37 ± 0.11 mg mL⁻¹ and 5.59 ± 0.09 mg mL⁻¹, respectively. Molecular simulation indicated that PDL and SVGGAL bind to XOD mainly through hydrogen bond and hydrophobic interaction, thereby inhibiting XOD activity. The research results suggested that the two peptides had potential application prospects as a safe XOD inhibitor substance for hyperuricemia treatment.

Keywords: *Auxis thazard* hydrolysate (ATH), XOD inhibiting peptides, identification, molecular docking.

Practical applications: This research not only effectively improves the utilization value of *Auxis thazard*, but also provide theoretical evidence in support of *Auxis thazard* peptides as a dietary supplement in hyperuricemic treatment.

1 Introduction

Hyperuricemia (HUA) is a metabolic disease caused by the overproduction and insufficient excretion of uric acid (UA) (George & Minter, 2021). It is well known as a factor for stone gout, inflammatory reaction and kidney injury diseases (Borghetti et al., 2020; Ponticelli et al., 2020). As a the end product of purine, UA is mainly regulated by the xanthine oxidase (XOD) in liver, which participates in catalyzing xanthine or hypoxanthine further into UA (Maiuolo et al., 2016). Therefore, XOD is considered as one of the targets for the treatment of hyperuricemia.

Some drugs were commonly used to treat hyperuricemia in clinical medicine, such as allopurinol and febuxostat (XOD inhibitor). However, these drugs easily induced adverse side effects (Liu et al., 2019a; Martens et al., 2020; Ying, 2020). Consequently, it is necessary to develop some natural and nontoxic products that possess XOD inhibitory activity. In recent years,

bioactive peptides with XOD inhibitory activity have attracted much attentions for researchers due to their easy absorption, nontoxicity and rich nutrition (Abd El-Salam & El-Shibiny, 2020; Jang et al., 2014). Some food derived-peptides with XOD inhibitory activity have also been isolated from milk protein (Nongonierma & Fitzgerald, 2012), shark-cartilage (Murota et al., 2014), tuna protein and walnut (He et al., 2019; Li et al., 2018a). Moreover, there is a growing interest in discovering functions of bioactive peptides, including antioxidative activity (Sipahli et al., 2021), ACE inhibitory activity (Gaspar-Pintilieșcu et al., 2019),

anticancer activity (Ramkisson et al., 2020), anti-inflammatory activity, DPP-IV inhibitory (Ji et al., 2021) and so far, which contribute to several physiological and functional roles in human body (Rafiq et al., 2020; Sosalagere et al., 2022).

Auxis thazard, also named bonito, is a kind of deep-sea migratory and low-value tuna, mainly distributed in the east and south sea of China (Chen & Xin-jun, 2017). It had various biological activities due to its high content of carnosine and anserine. Previous research proved that bonito peptides had the functions of antioxidant, reducing uric acid and inhibiting XOD (Kikuchi et al., 2004; Sri Kantha et al., 2000; Otsuka et al., 2016). However, the XOD inhibitory peptides from *Auxis thazard* and their interaction mechanism was seldom reported.

The objective of this study is to purify xanthine oxidase inhibitory peptides from ATH, identify their amino acids sequence and to investigate interaction mechanisms between the peptides and XOD via molecular docking.

2 Materials and methods

2.1 Materials and reagents

The *Auxis thazard* was purchased from Guangdong Xingyi Marine Biological Technology Co. Ltd. (Guangzhou, China). Alcalase was produced from Pangbo Biotech Co. Ltd (Nanning,

Received 08 Oct., 2021

Accepted 09 Dec., 2021

¹ College of Food Science and Technology, Guangdong Ocean University, Zhanjiang, China

² Guangdong Provincial Key Laboratory of Aquatic Product Processing and Safety, Zhanjiang, China

³ Guangdong Province Engineering Laboratory for Marine Biological Products, Zhanjiang, China

⁴ Guangdong Provincial Engineering Technology Research Center of Marine Food, Zhanjiang, China

⁵ Key Laboratory of Advanced Processing of Aquatic Product of Guangdong Higher Education Institution, Zhanjiang, China

⁶ Collaborative Innovation Center of Seafood Deep Processing, Dalian Polytechnic University, Dalian, China

*Corresponding author: jihw62318@163.com

China). Xanthine oxidase, xanthine and acetonitrile were purchased from Sigma-Aldrich (Saint Louis, MO, US). Ultrafiltration membrane and Sephadex gel were purchased from GE Company (Boston, US).

2.2 Preparation of ATH

The ATH was prepared as follows (Chen et al., 2019), the *Auxis thazard* meat was homogenized and enzymatically hydrolyzed for 5 h under certain conditions (temperature 60 °C, pH 8.0, the solid-liquid ratio of 1:3, adding alkaline protease 500 U per gram protein). Then, the termination of the hydrolysis reaction was boiled at 100°C for 15 min. The enzymatic hydrolyte was centrifuged at 8000 rpm, 4 °C for 20 min, and the bonito hydrolytic supernatant (BH) was got after de-oiled with the absorbent cotton gauze. The bonito hydrolytic supernatant (BH) were filtered by the ceramic membrane (pore size 0.2 µm) and the 10, 5, 1 kDa M.W. cut-off ultrafiltration membrane, and the interception and permeating solutions was collected. There were separated into four ultrafiltration fractionation (UF), i.e., UF-1 (>10 kDa), UF-2 (5-10 kDa), UF-3 (1-5 kDa), UF-4 (<1 kDa). Finally, each ultrafiltration fractionation was obtained by the concentration and spray drying.

2.3 Methods

Determination of the XOD inhibitory activity of ATH

The experimental method is referenced from the literature (Masuda et al., 2019), with some modifications. The mixture 50 µL of the sample and 50 µL of 0.05 U mL⁻¹ XOD solution were added into 96 well plate that was shaken for 30 s and incubated at 25 °C for 5 min. Then, 150 µL of 0.48 Mmol L⁻¹ xanthine solution was added, and the mixture was shaken 30 s and incubated at 25 °C for 25 min. The absorbance at 290 nm was measured. The XOD inhibitory activity was calculated according to following Equation 1:

$$\text{Inhibition percentage (\%)} = \left(1 - \frac{A_1 - A_2}{A_3 - A_4}\right) \times 100\% \quad (1)$$

Where A_1 is the absorbance value of the production with the sample and XOD, A_2 is the absorbance of the production with the sample, A_3 is the absorbance the production with the buffer solution and XOD, and A_4 is the absorbance of the production with the buffer solution. The extent of inhibition was expressed as the IC₅₀.

Determination of the molecular weight distribution of ATH

The experimental method is referenced from the literature (Li et al., 2018a). The molecular weight (MW) distribution of ATO was monitored by a TSK gel G2000SWxL analytical column (30 cm*7.8 mm, Tosoh Corporation, Tokyo, Japan) attached to the Agilent HPLC system (Santa Clara, California, US). The mobile phase volume ratio of acetonitrile/water and trifluoroacetic acid was 45:55:0.1, the flow rate was set as 0.5 mL min⁻¹ (column temperature: 30 °C, running time: 30 min).

The calibration curve was obtained using the following standards from Yuanye Co. (Shanghai, China): Cytochrome C (12384 Da), aprotinin (6511.44 Da), bacitracin (1423 Da), oxidized glutathione (612.63 Da), Gly-Gly-Tyr-Arg (451 Da), Gly-Gly-Gly (189 Da), Absorbance at 220 nm was measured.

Analysis of hydrolytic amino acids of ATH

The experimental method is referenced from the literature (Chen et al., 2019). The sample was hydrolyzed by 6.0 mol L⁻¹ HCl, and 17 amino acids were analyzed by Hitachi 835-50 high-speed amino acid analyzer. In addition, the sample was hydrolyzed by 5.0 mol L⁻¹ NaOH, and the content of tryptophan was analyzed on the same machine.

Separation of ATH by Sephadex G-15

The experimental method is referenced from the literature (He et al., 2019). The UF-4 with highest XOD inhibitory activity was separated via size-exclusion chromatography using the AKTA protein purification system (Boston, USA) with the Sephadex G-15 column (60 cm * 16 mm, Boston, USA). The lyophilized sample of UF-4 (15 mg mL⁻¹) was eluted with distilled water at a flow rate of 1.0 mL min⁻¹ and a loading volume of 1.0 mL. Then, all fractions were detected at 214 nm and collected for further study.

Purification of ATH by reversed-phase high-performance liquid chromatography

The experimental method is referenced from the literature (He et al., 2019). The F2 with highest XOD inhibitory activity thus was chosen for further separation by the reversed-phase high-performance liquid chromatography (RT-HPLC) with the Synergi Hydro-RP analytical column (150 * 10 mm, Japan). The F2 (5 mg mL⁻¹) was eluted with the mobile phase consisting of distilled water (containing 0.1% trifluoroacetic acid) (A) and acetonitrile (B) at the flow rate of 2 mL min⁻¹ with a loading volume of 20 µL in gradient mode: 100% A at 0-5 min; 100-70% A at 6-12 min; 70-100% A at 13-16 min; 100% A at 17-20 min. Then, all fractions were detected at 214 nm and collected for further study.

Identification of peptides by UPLC-MS/MS

The experimental method is referenced from the literature (Chen et al., 2019). Samples were (10.0 µg mL⁻¹, dissolved in 20% acetonitrile and distilled water) were detected via mass spectrometry (MS, Waters, US), which was filled with a C18 column (2.1*150 mm, 1.7 µm). The mobile phase consisted of solutions distilled water (containing 0.1% formic acid) (A) and acetonitrile (B) at the flow rate of 0.2 mL min⁻¹ with a loading volume of 10 µL, and the elution was set as follows: 98% A at 0-2 min; 98-60% A at 3-5 min; 60-98% A at 5.5-7 min. The spray temperature and MS/MS voltage source were set as 400 °C and 25 kV, respectively. Finally, the peptide sequencing was performed through proceeding the MS/MS spectra via Compass Data Analysis software (Version4.1, Bruker Daltonik GmbH) and manual calculation.

Molecule docking study

Molecule docking of peptide-XOD complex was conducted to explore the effect of lowering UA by peptide (Li et al., 2019). Thus, Discovery studio 4.5 software (Biovia Inc., San Diego, US) was used to examine the interaction of peptide with the active site of XOD. Firstly, the peptides structure was drawn with Chem3D 15.1 software and saved in mol2 format. The X-ray crystal structure of bovine XOD (3NVY) was downloaded from RCSB Protein Data Bank (<https://www.rcsb.org/pdb>). The receptor protein (3NVY) was repaired by discovery studio 2019, the procedures including cleaning, removing the inhibitor and water, adding hydrogen (Zhang et al., 2017), and the molecular docking results were analyzed by Pymol and DS4.5 software.

2.4 Statistical analysis

The data are presented as means \pm standard deviation and statistically analyzed by Graph Pad Prism 7.0 software (San Diego, CA, US). Significant differences between groups were judged by One-way analysis of variance (ANOVA), followed by Multiple comparisons test. Differences were significant when $p < 0.05$.

3 Results and discussion

3.1 The XOD inhibitory activity of ATH

The XOD inhibitory activity of ATH were shown in (Figure 1A). From the Figure 1A, it can be seen that the XOD inhibitory activity of UF-4 ($IC_{50} = 11.23 \pm 0.31 \text{ mg mL}^{-1}$) was remarkably higher than other fractionations ($p < 0.05$). Compared with the original bonito hydrolytic supernatant ($IC_{50} = 14.47 \pm 0.70 \text{ mg mL}^{-1}$),

the IC_{50} value of UF-4 was remarkably down 22.38% ($p < 0.05$). The IC_{50} values of UF-1, UF-2, UF-3 were 20.50 mg mL^{-1} , 17.23 mg mL^{-1} , 13.67 mg mL^{-1} , respectively. Those results suggested that ATH possessed significant XOD inhibitory effect in vitro. Previous research proved that the 600-800 Da ultrafiltration fractionation had obvious XOD inhibitory activity (the IC_{50} value was 9.18 mg mL^{-1}), which was 38.31% lower than the original skipjack tuna hydrolysate (Zhong et al., 2021).

3.2 Molecular weight distribution and amino acid composition of ATH

The diverse molecular weight often make different functional activities. It was reported that peptides with small MW ($< 1 \text{ kDa}$) was easier absorption and exhibited biological activities (Wang et al., 2020). The UF-4 with highest XOD inhibitory activity was used for further determination of amino acid composition and molecular weight distribution. According to the size exclusion chromatogram of standards (Figure 1B) and the molecular weight distribution curve of standards (Figure 1C), it can be seen that almost 95% of the molecular weight of UF-4 is mainly distributed in 180 Da-1000 Da (Figure 1D), which indicating that ATH could have the potential bioactivity. The biological activities of peptides in ATH are mainly related to their structural features, such as amino acid composition, sequence, hydrophobicity (Navarro-Peraza et al., 2020). It was reported that the hydrophobic amino acids were positively related to XOD inhibitory activity (He et al., 2019; Li et al., 2019; Murota et al., 2014). The amino acids composition of UF-4 of ATH is shown in Table 1, the total content of hydrolyzed amino acids was $66.9 \text{ g}/100 \text{ g}$, the hydrophobic amino acids accounts for 31.81%. In addition, the

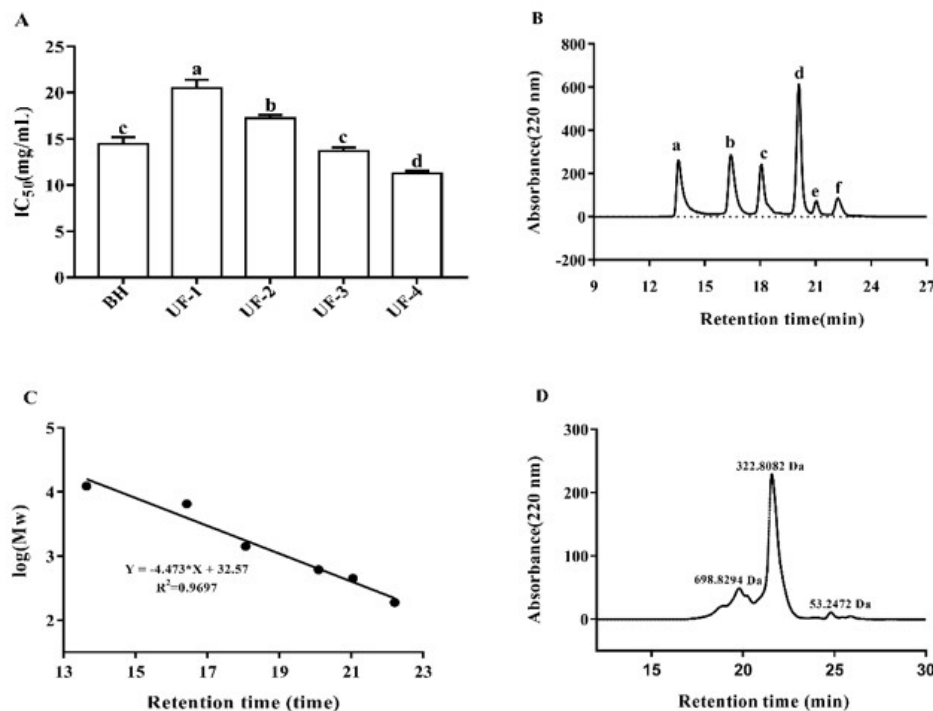


Figure 1. The (A) XOD inhibitory activity of ATH, (B) the size exclusion chromatogram of standards, (C) molecular weight distribution curve of standards and (D) the molecular weight distribution of ATH (All data are mean \pm standard deviation, significant difference was shown at $p < 0.05$).

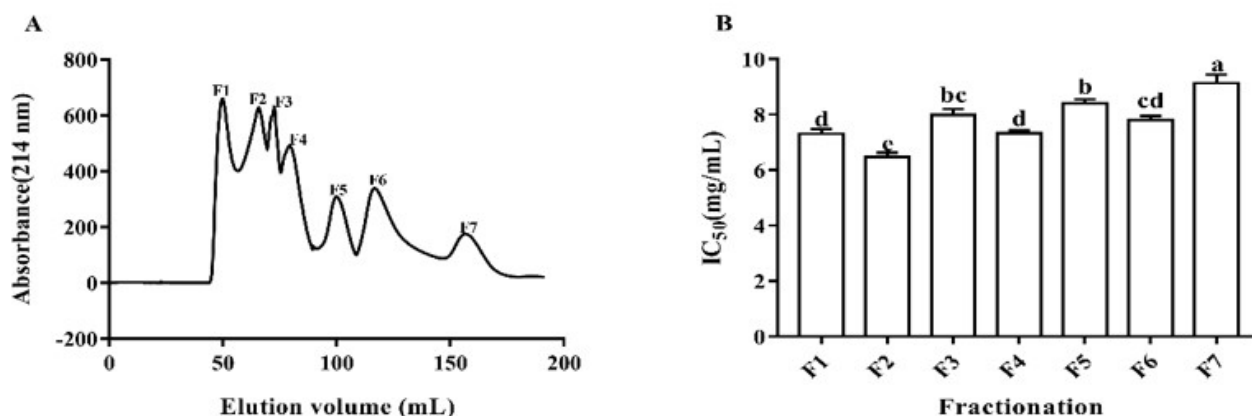


Figure 2. Elution volume of the ATH on (A) Sephadex G-15 column (1.6*70 cm) at 214 nm and (B) the IC₅₀ value of XOD inhibitory activity in seven fractions separated from Sephadex G-15.

Table 1. Amino acid composition of ATH.

Amino acid	Content (g/100 g)	Amino acid	Content (g/100 g)
Asp	5.34 ± 0.11	Met	2.31 ± 0.12
Thr	3.26 ± 0.20	Ile	2.66 ± 0.26
Ser	2.60 ± 0.15	Leu	6.0 ± 0.07
Glu	8.95 ± 0.12	Tyr	1.96 ± 0.1
Pro	1.99 ± 0.09	Phe	2.37 ± 0.4
Gly	3.23 ± 0.21	Lys	7.04 ± 0.07
Ala	4.64 ± 0.12	His	7.28 ± 0.06
Val	3.3 ± 0.14	Arg	3.37 ± 0.06

Note: All data are mean ± standard deviation.

content of essential amino acids was 25.30 g/100 g. These results indicated that ATH has potential uric acid-lowering activity and comprehensive nutrition.

3.3 Sephadex G-15 separation and evaluation of XOD inhibitory activity

The size exclusion chromatography was applied for elution and separation of biological macromolecules according to molecules size. In this study, Sephadex G-15 was used for separating peptides with MW below 1500 Da. As shown in Figure 2A, UF-4 with the highest XOD inhibitory activity was separated into seven fractions F₁, F₂, F₃, F₄, F₅, F₆ and F₇ by G-15. The XOD inhibitory activity of these seven fractions were shown in Figure 2B, the XOD inhibitory activity of F₂ was highest, followed by F₁, F₄, F₆, F₃, F₅ and F₇. Among them, the IC₅₀ value of F₂ were 6.46 ± 0.13 mg mL⁻¹, which was lower 42.48% than the UF-4 (IC₅₀ = 11.23 ± 0.31 mg mL⁻¹). XOD inhibitory peptides had been purified from the bonito by Sephadex G-15 and Superdex peptide GL 10/300 in previous research and showed that the peptide containing Phe exhibited stronger XOD inhibiting activity. (He et al., 2019; Yujuan, 2019). Thus, based on the current results, the F₂ was regarded as the major component to be further investigated in the XOD inhibitor activity.

3.4 RT-HPLC purification and evaluation of XOD inhibitory activity

The RP-HPLC method is a highly sensitive and rapid method, which is typically used for the purification of small molecules, particularly those with MW below 1 kDa (Garcia et al., 2006). In this study, the F₂ fraction with highest XOD inhibitory activity obtained by Sephadex G-15 gel separation was further purified via RT-HPLC, and two absorption peaks were obtained, i.e., F₂₋₁, F₂₋₂ (Figure 3A). The XOD inhibitory activity of two fractions were shown in (Figure 3B), the IC₅₀ value of the F₂₋₁ and F₂₋₂ were detected to be 4.37 ± 0.11 mg mL⁻¹ and 5.59 ± 0.09 mg mL⁻¹, respectively. It has been reported that the peptides from rice shell protein purified by gel filtration and HPLC had XOD inhibitory activity, whose inhibition rate was 3/4 of that of allopurinol (Liu et al., 2020a). The IC₅₀ value of XOD inhibitory peptides purified from tilapia hydrolysate was 4.51 mg mL⁻¹ (Zhouhuang, 2018). Two novel anti-hyperuricemic peptides derived Walnut protein displayed high in vitro XOD inhibitory activity with the IC₅₀ values of 17.75 ± 0.12 mg mL⁻¹ (WPPKN) and 19.01 ± 0.23 mg mL⁻¹ (ADIYTE) (Li et al., 2018a). To elucidate the relationship between the inhibit XOD activity and primary peptide structure of F₂₋₁, F₂₋₂, the UPLC-MS/MS was used to further identify its peptide sequences.

3.5 Identification of peptides via UPLC-MS/MS

The fractions F₂₋₁ and F₂₋₂ with the higher XOD inhibitory activity were analyzed by mass spectrometry, As shown in Figure 4A-B, the two peptides parent ions with m/z at 344.8770 (F₂₋₁) and 504.2662 (F₂₋₂) were selected for fragmentation via the software of the MS spectrometer. At present, the analysis of structure of peptide sequence is mainly based on the naming system proposed by roepsstorff and fohlman. Generally, the fragment ions can be divided into two types: a, b and c are represented by the N-terminal fragment ions, and x, y and z are represented by the C segment; Among them, b and y fragment ions are considered to be the key to judge the peptide sequence (Craig et al., 1993; Smith et al., 1991).

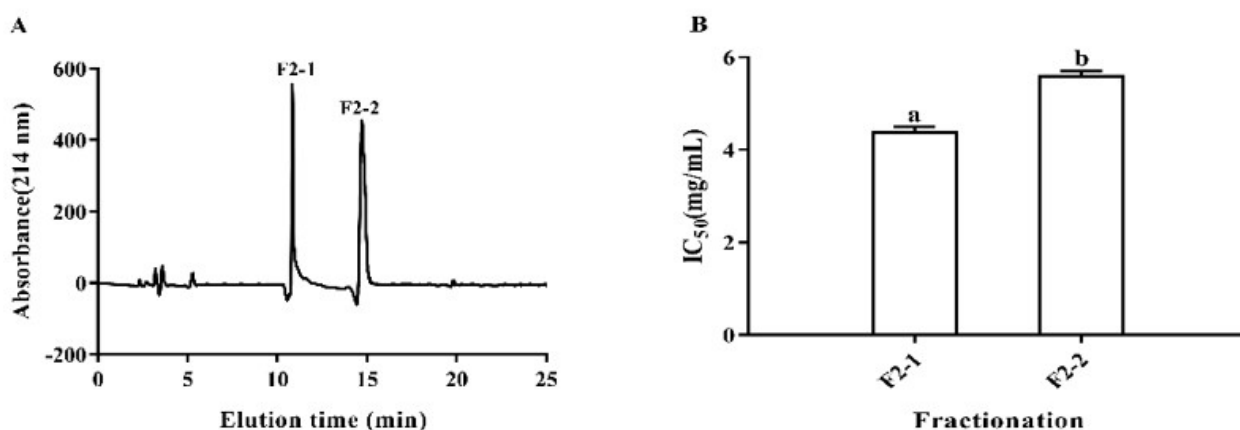


Figure 3. Purification of ATH by RP-HPLC (A) fraction F₂ derived from G-15 and (B) the IC₅₀ value of XOD inhibitory activity in F₂₋₁ and F₂₋₂ separated from RP-HPLC.

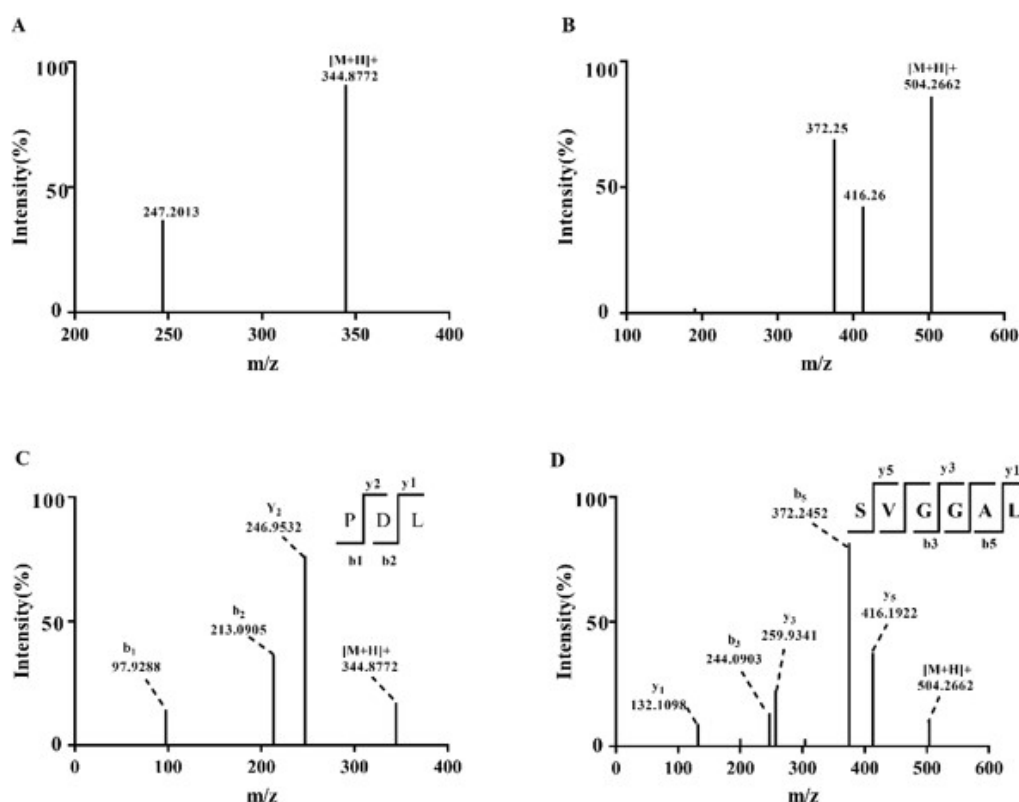


Figure 4. Identification of molecular mass and amino acid sequence of ATH, the MS spectrum of purified fraction (A) F₂₋₁ and (B) F₂₋₂; the amino acid sequence of purified fraction (C) F₂₋₁ and (D) F₂₋₂.

According to the fragmentation and the fracture mode of the peptide chain, the amino acid sequence of parent ion m/z at 344.8770 could be determined. As shown in Figure 4C, the $m/z = 213.9005$ peak was for b_2 ion, which corresponded to the mass of fragment Pro-Asp-, and the m/z at 246.9532 was for y_2 ion (probably fragment Asp-Leu-). Similarly, the b_1 ions corresponded to proline residue. The MS/MS sequence of charged ions with m/z at 504.2662 were illustrated in Figure 4D, it can

be seen that the m/z at 132.1098 was for the y_1 ion, and the $m/z = 244.0903$ peak was for the b_3 ion (probably fragment Ser-Val-Gly-). The y_3 ion with $m/z = 259.9341$ corresponded to the fragment Gly-Ala-Leu-. Meanwhile, the $m/z = 372.2452$ peak was for b_5 ion (probably fragment Ser-Val-Gly-Gly-Ala-); and the m/z at 416.1922 peak was for y_5 ion (probably fragment Val-Gly-Gly-Ala-Leu-). So based on these results, the sequences of two peptides were identified to be Pro-Asp-Leu (PDL) and

Ser-Val-Gly-Gly-Ala-Leu (SVGGAL) with molecular weight of 304.87 Da and 504.26 Da, respectively.

To our knowledge, the XOD activity was affected not only by the molecular weight of the peptides but also by the amino acid sequence of the peptides. It was reported that food-derived XOD inhibitory peptides were usually composed of 2 - 10 amino acids with molecular weight less than 1000 Da. Generally, aromatic amino acids (such as Trp, Tyr, Phe and His) and hydrophilic amino acids located at the N-end of peptides possessed higher XOD inhibitory activity than the C-end. However, polypeptides with aromatic amino acids located in the middle was not conducive to exert XOD inhibitory activity. Besides, hydrophobic amino acids located at the C-terminal of the polypeptide could promote XOD inhibitory activity (He et al., 2019; Jang et al., 2014; Li et al., 2018a, b; Liu et al., 2019b, 2020a, b; Murota et al., 2014; Nongonierma & Fitzgerald, 2012; Wan et al., 2020; Zhong et al., 2021). In this study, two peptides was identified with molecular weight of 304.87 Da and 504.26 Da and hydrophobic amino acids located at the C-terminal, and this result was also in agreement above report. However, the amino acid sequence of two peptides had not been reported up to now. Hence, the molecular dock was used to investigate the relationship between the peptide and XOD activity.

3.6 Molecular dock studying of the peptide and XOD

Molecular docking can be used to predict the structural interaction between ligand and receptor. According to the docking law of discovery studio, if value of energy was lower, it indicated that the docking system of receptor and ligand was more stable (Zhang et al., 2015). According to the report, some amino acid residues can affect the active center of XOD including Phe649, Phe914, Phe1009, Asn768, Val1011, Glu802, Ser876, Lys771, Leu873, Leu1014, Arg880, Thr1010 and Glu126 (Nishino et al., 2008). The interactions between PDL and XOD activity were showed in Figure 5A and C, and the estimated lowest binding energy was -7.89 kcal/mol. The amino acid residues around the binding of PDL to XOD were Asn768, Ser876, His875, Glu802, Leu873, Lys771, Glu802, Phe914, Thr803, Pro1076, Thr1010, Arg880, Ala1079, Ala1078, Ala910, Phe1009, Leu1014, Asp872, Phe649, Phe1013 and Val1011. As seen in the Table 2, PDL forms hydrogen bonds with the amino acid residues Asn768, Ser876, Leu873, Glu802 with bond lengths of 2.2, 3.0, 3.4, and 2.0 Å, respectively. Moreover, eleven van der Waals and four hydrophobic interaction were observed in those amino acid residues.

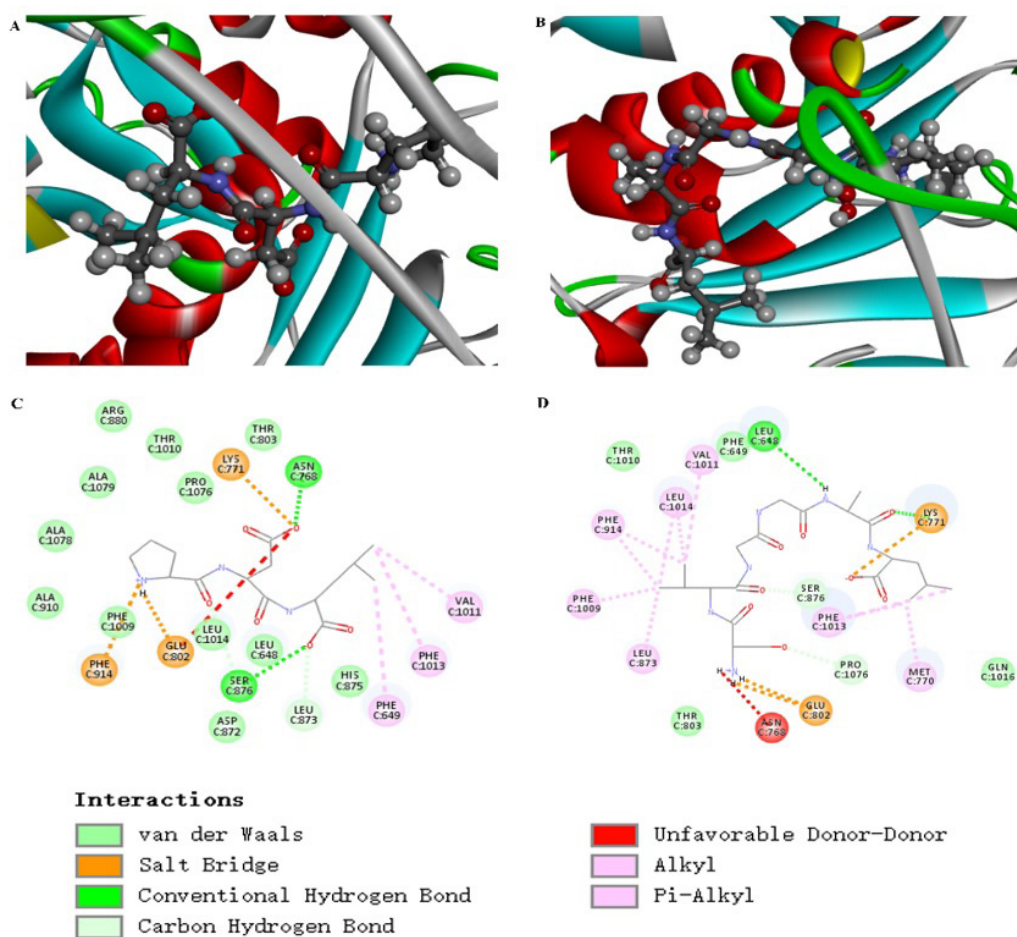


Figure 5. Molecular docking simulation of the PDL and SVGGAL peptide with XOD (3NVY), the 3D structural analysis of XOD with (A) PDL and (B) SVGGAL; the 2D structural analysis of XOD with (C) PDL and (D) SVGGAL.

Table 2. The docking results of target protein with peptides.

Receptor	Ligand	Binding energy (kcal/mol)	Contact sites		
			Hydrogen bond interaction	Van der Waals interaction	Hydrophobic interaction
3NVY	PDL	-7.89	Asn768	Thr803, Pro1076	Phe914, Val1011
			Ser876	Thr1010, Arg880	Phe649, Phe1013
			Leu873	Ala1079, Ala1078	
			Glu802	Ala910, Phe1009	
3NVY	SVGGAL	-7.28		Leu1014, Leu648	
			Asn768	Thr1010, Phe649	Val1011, Met770
			Glu802	Gln1016, Thr803	Phe914, Phe1009
			Leu648		Leu873, Leu1014
			Lys771		Phe1013

The docking results of SVGGAL was illustrated in Figure 5B and D, and the estimated lowest binding energy was -7.28 kcal/mol. Those amino acid residues appeared around the binding of SVGGAL to XOD including Leu648, Asn768, Glu802, Lys771, Phe649, Val1011, Leu1014, Phe914, Phe1009, Leu873, Thr803, Ser876, Phe1013, Met770, Gln1016. As seen in the Table 2, four hydrogen bonds were found, including Asn768, Glu802, Leu648, Lys771 with bond lengths of 1.8, 2.5, 2.5, and 1.9 Å, respectively. Some researchers showed that Asn768, Glu802, Lys771 residues could contribute to catalytic XOD inhibitor activity, among them Lys771 residues was located next to the Mo domain (Ichida et al., 2012; Li et al., 2018a). Besides, there were van der Waals interactions with Thr1010, Phe649, Gln1016, Thr803, and even hydrophobic amino acid residues. Based on this, it is speculated that PDL and SVGGAL binds to XOD mainly through hydrogen bond, van der Waals force and hydrophobic force to inhibit the catalytic activity of XOD.

4 Conclusion

In this study, two peptides with high XOD inhibitory activity have been purified from ATH and identified as Pro-Asp-Leu (PDL) and Ser-Val-Gly-Gly-Ala-Leu (SVGGAL), which possessed XOD inhibitory activity with the IC_{50} values of 4.37 ± 0.11 mg mL⁻¹ and 5.59 ± 0.09 mg mL⁻¹, respectively. Molecular simulation indicated that PDL and SVGGAL contributed inhibition effects by inserting into the active center of XOD. The research results suggested that the two peptides had potential application prospects as a safe XOD inhibitor substance for hyperuricemia treatment.

Conflict of interest

The authors declare that they have no conflict of interest.

Acknowledgements

This work was supported by the National Key Research and Development Program (2019YFD0902004).

References

Abd El-Salam, M. H., & El-Shibiny, S. (2020). Milk fat globule membrane: an overview with particular emphasis on its nutritional and health

benefits. *International Journal of Dairy Technology*, 73(4), 639-655. <http://dx.doi.org/10.1111/1471-0307.12730>.

Borghi, C., Agabiti-Rosei, E., Johnson, R. J., Kielstein, J. T., Lurbe, E., Mancia, G., Redon, J., Stack, A. G., & Tsioufis, K. P. (2020). Hyperuricaemia and gout in cardiovascular, metabolic and kidney disease. *European Journal of Internal Medicine*, 80, 1-11. <http://dx.doi.org/10.1016/j.ejim.2020.07.006>. PMID:32739239.

Chen, M., Ji, H., Zhang, Z., Zeng, X., Su, W., & Liu, S. (2019). A novel calcium-chelating peptide purified from Auxis thazard protein hydrolysate and its binding properties with calcium. *Journal of Functional Foods*, 60, 103447. <http://dx.doi.org/10.1016/j.jff.2019.103447>.

Chen, Y., & Xin-jun, C. (2017). Reviews on Skipjack (*Katsuwonus pelamis*) fishery in the west-central pacific ocean. *Journal of Guangdong Ocean University*, 37(5), 34-43.

Craig, A. G., Koerber, S. C., Rivier, J. E., & Bennich, H. (1993). A strategy to assign a series of fragment ions: investigation of fragment ions involving peptide side chain and backbone cleavage. *International Journal of Mass Spectrometry and Ion Processes*, 126(29), 137-149. [http://dx.doi.org/10.1016/0168-1176\(93\)80078-S](http://dx.doi.org/10.1016/0168-1176(93)80078-S).

Garcia, J., Far, S., Diesis, E., & Melnyk, O. (2006). Determination of glyoxylyl-peptide concentration using oxime chemistry and RP-HPLC analysis. *Journal of Peptide Science*, 12(11), 734-738. <http://dx.doi.org/10.1002/psc.791>. PMID:16981231.

Gaspar-Pintiliecu, A., Oancea, A., Cotarlet, M., Vasile, A. M., Bahrim, G. E., Shaposhnikov, S., Craciunescu, O., & Oprita, E. I. (2019). Angiotensin-converting enzyme inhibition, antioxidant activity and cytotoxicity of bioactive peptides from fermented bovine colostrum. *International Journal of Dairy Technology*, 73(1), 108-116. <http://dx.doi.org/10.1111/1471-0307.12659>.

George, C., & Minter, DA. (2021). *Hyperuricemia*. Treasure Island: StatPearls.

He, W., Su, G., Sun-Waterhouse, D., Waterhouse, G. I. N., Zhao, M., & Liu, Y. (2019). In vivo anti-hyperuricemic and xanthine oxidase inhibitory properties of tuna protein hydrolysates and its isolated fractions. *Food Chemistry*, 272, 453-461. <http://dx.doi.org/10.1016/j.foodchem.2018.08.057>. PMID:30309568.

Ichida, K., Amaya, Y., Okamoto, Y. A. K., & Nishino, T. (2012). Mutations associated with functional disorder of xanthine oxidoreductase and hereditary xanthinuria in humans. *International Journal of Molecular Sciences*, 13(11), 15475-15495. <http://dx.doi.org/10.3390/ijms131115475>. PMID:23203137.

Jang, I. T., Hyun, S. H., Shin, J. W., Lee, Y. H., Ji, J. H., & Lee, J. S. (2014). Characterization of an Anti-gout Xanthine Oxidase Inhibitor from

- Pleurotus ostreatus. *Mycobiology*, 42(3), 296-300. <http://dx.doi.org/10.5941/MYCO.2014.42.3.296>. PMID:25346610.
- Ji, W., Zhang, C., Song, C., & Ji, H. (2021). Three DPP-IV inhibitory peptides from Antarctic krill protein hydrolysate improve glucose levels in the zebrafish model of diabetes. *Food Science and Technology*. Ahead of Print. <http://dx.doi.org/10.1590/fst.58920>.
- Kikuchi, K., Matahira, Y., & Sakai, K. (2004). Separation and physiological functions of anserine from fish extract. *Developments in Food Science*, 42, 97-105. [http://dx.doi.org/10.1016/S0167-4501\(04\)80012-8](http://dx.doi.org/10.1016/S0167-4501(04)80012-8).
- Li, Q., Kang, X., Shi, C., Li, Y., Majumder, K., Ning, Z., & Ren, J. (2018a). Moderation of hyperuricemia in rats via consuming walnut protein hydrolysate diet and identification of new antihyperuricemic peptides. *Food & Function*, 9(1), 107-116. <http://dx.doi.org/10.1039/C7FO01174A>. PMID:29019366.
- Li, Q., Shi, C., Wang, M., Zhou, M., Liang, M., Zhang, T., Yuan, E., Wang, Z., Yao, M., & Ren, J. (2019). Tryptophan residue enhances in vitro walnut protein-derived peptides exerting xanthine oxidase inhibition and antioxidant activities. *Journal of Functional Foods*, 53, 276-285. <http://dx.doi.org/10.1016/j.jff.2018.11.024>.
- Li, Y., Kang, X., Li, Q., Shi, C., Lian, Y., Yuan, E., Zhou, M., & Ren, J. (2018b). Anti-hyperuricemic peptides derived from bonito hydrolysates based on in vivo hyperuricemic model and in vitro xanthine oxidase inhibitory activity. *Peptides*, 107, 45-53. <http://dx.doi.org/10.1016/j.peptides.2018.08.001>. PMID:30077718.
- Liu, C. W., Chang, W. C., Lee, C. C., Shau, W. Y., Hsu, F. S., Wang, M. L., Chen, T. C., Lo, C., & Hwang, J. J. (2019a). The net clinical benefits of febuxostat versus allopurinol in patients with gout or asymptomatic hyperuricemia: a systematic review and meta-analysis. *Nutrition, Metabolism, and Cardiovascular Diseases*, 29(10), 1011-1022. <http://dx.doi.org/10.1016/j.numecd.2019.06.016>. PMID:31378626.
- Liu, N., Meng, B., Zeng, L., Yin, S., Hu, Y., Li, S., Fu, Y., Zhang, X., Xie, C., Shu, L., Yang, M., Wang, Y., & Yang, X. (2020a). Discovery of a novel rice-derived peptide with significant anti-gout potency. *Food & Function*, 11(12), 10542-10553. <http://dx.doi.org/10.1039/D0FO01774D>. PMID:33185232.
- Liu, N., Wang, Y., Yang, M., Bian, W., Zeng, L., Yin, S., Xiong, Z., Hu, Y., Wang, S., Meng, B., Sun, J., & Yang, X. (2019b). New rice-derived short peptide potently alleviated hyperuricemia induced by potassium oxonate in rats. *Journal of Agricultural and Food Chemistry*, 67(1), 220-228. <http://dx.doi.org/10.1021/acs.jafc.8b05879>. PMID:30562028.
- Liu, N., Wang, Y., Zeng, L., Yin, S., Hu, Y., Li, S., Fu, Y., Zhang, X., Xie, C., Shu, L., Li, Y., Sun, H., Yang, M., Sun, J., & Yang, X. (2020b). RDP3, a novel antigout peptide derived from water extract of rice. *Journal of Agricultural and Food Chemistry*, 68(27), 7143-7151. <http://dx.doi.org/10.1021/acs.jafc.0c02535>. PMID:32543191.
- Maiuolo, J., Oppedisano, F., Gratteri, S., Muscoli, C., & Mollace, V. (2016). Regulation of uric acid metabolism and excretion. *International Journal of Cardiology*, 213, 8-14. <http://dx.doi.org/10.1016/j.ijcard.2015.08.109>. PMID:26316329.
- Martens, K. L., Khalighi, P. R., Li, S., White, A. A., Silgard, E., Frieze, D., Estey, E., Garcia, D. A., Hingorani, S., & Li, A. (2020). Comparative effectiveness of rasburicase versus allopurinol for cancer patients with renal dysfunction and hyperuricemia. *Leukemia Research*, 89, 106298. <http://dx.doi.org/10.1016/j.leukres.2020.106298>. PMID:31945598.
- Masuda, T., Fukuyama, Y., Doi, S., Masuda, A., Kurosawa, S., & Fujii, S. (2019). Effects of temperature on the composition and Xanthine oxidase inhibitory activities of caffeic acid roasting products. *Journal of Agricultural and Food Chemistry*, 67(32), 8977-8985. <http://dx.doi.org/10.1021/acs.jafc.9b03633>. PMID:31334649.
- Murota, I., Taguchi, S., Sato, N., Park, E. Y., Nakamura, Y., & Sato, K. (2014). Identification of antihyperuricemic peptides in the proteolytic digest of shark cartilage water extract using in vivo activity-guided fractionation. *Journal of Agricultural and Food Chemistry*, 62(11), 2392-2397. <http://dx.doi.org/10.1021/jf405504u>. PMID:24588444.
- Navarro-Peraza, R. S., Osuna-Ruiz, I., Lugo-Sánchez, M. E., Pacheco-Aguilar, R., Ramírez-Suárez, J. C., Burgos-Hernández, A., Martínez-Montaño, E., & Salazar-Leyva, J. A. (2020). Structural and biological properties of protein hydrolysates from seafood by-products: a review focused on fishery effluents. *Food Science and Technology*, 40(Suppl. 1), 1-5. <http://dx.doi.org/10.1590/fst.24719>.
- Nishino, T., Okamoto, K., Eger, B. T., Pai, E. F., & Nishino, T. (2008). Mammalian xanthine oxidoreductase: mechanism of transition from xanthine dehydrogenase to xanthine oxidase. *The FEBS Journal*, 275(13), 3278-3289. <http://dx.doi.org/10.1111/j.1742-4658.2008.06489.x>. PMID:18513323.
- Nongonierma, A. B., & Fitzgerald, R. J. (2012). Tryptophan-containing milk protein-derived dipeptides inhibit xanthine oxidase. *Peptides*, 37(2), 263-272. <http://dx.doi.org/10.1016/j.peptides.2012.07.030>. PMID:22910190.
- Otsuka, Y., Ohno, Y., Morita, A., Otani, N., Jutabha, P., Ouchi, M., Tsuruoka, S., & Anzai, N. (2016). Molecular mechanism of urate-lowering effect of anserine hitrate. *Gout and Nucleic Acid Metabolism*, 40(2), 137-143. <http://dx.doi.org/10.6032/gnam.40.137>.
- Ponticelli, C., Podesta, M. A., & Moroni, G. (2020). Hyperuricemia as a trigger of immune response in hypertension and chronic kidney disease. *Kidney International*, 98(5), 1149-1159. <http://dx.doi.org/10.1016/j.kint.2020.05.056>. PMID:32650020.
- Rafiq, S., Gulzar, N., Sameen, A., Huma, N., Hayat, I., & Ijaz, R. (2020). Functional role of bioactive peptides with special reference to cheeses. *International Journal of Dairy Technology*, 74(1), 1-16. <http://dx.doi.org/10.1111/1471-0307.12732>.
- Ramkissoon, S., Dwarka, D., Venter, S., & Mellem, J. J. (2020). In vitro anticancer and antioxidant potential of Amaranthus cruentus protein and its hydrolysates. *Food Science and Technology*, 40(Suppl. 2), 634-639. <http://dx.doi.org/10.1590/fst.36219>.
- Sipahli, S., Dwarka, D., Amonsou, E., & Mellem, J. (2021). In vitro antioxidant and apoptotic activity of Lablab purpureus (L.) Sweet isolate and hydrolysates. *Food Science and Technology*. <http://dx.doi.org/10.1590/fst.55220>.
- Smith, J. B., Thévenon-Emeric, G., Smith, D. L., & Green, B. (1991). Elucidation of the primary structures of proteins by mass spectrometry. *Analytical Biochemistry*, 193(1), 118-124. [http://dx.doi.org/10.1016/0003-2697\(91\)90050-4](http://dx.doi.org/10.1016/0003-2697(91)90050-4). PMID:2042736.
- Sosalagere, C., Adesegun Kehinde, B., & Sharma, P. (2022). Isolation and functionalities of bioactive peptides from fruits and vegetables: A reviews. *Food Chemistry*, 366, 130494. <http://dx.doi.org/10.1016/j.foodchem.2021.130494>. PMID:34293544.
- Sri Kantha, S., Takeuchi, M., Watabe, S., & Ochi, H. (2000). HPLC determination of carnosine in commercial canned soups and natural meat extracts. *Lebensmittel-Wissenschaft + Technologie*, 33(1), 60-62. <http://dx.doi.org/10.1006/fstl.1999.0602>.
- Wan, H., Han, J., Tang, S., Bao, W., Lu, C., Zhou, J., Ming, T., Li, Y., & Su, X. (2020). Comparisons of protective effects between two sea cucumber hydrolysates against diet induced hyperuricemia and renal inflammation in mice. *Food & Function*, 11(1), 1074-1086. <http://dx.doi.org/10.1039/C9FO02425E>. PMID:31825427.
- Wang, P., Lin, Y., Wu, H., Lin, J., Chen, Y., Hamzah, S. S., Zeng, H., Zhang, Y., & Hu, J. (2020). Preparation of antioxidant peptides from hairtail surimi using hydrolysis and evaluation of its antioxidant stability. *Food Science and Technology*, 40(4), 945-955. <http://dx.doi.org/10.1590/fst.23719>.

- Ying, H. (2020). Research progress of drugs for hyperuricemia. *Journal of Jilin Medical College*, 41(5), 381-382.
- Yujuan, L. (2019). *Preparation, isolation, structural characterization, and the effect mechanism of uric acid-lowering peptides derived from bonito* (Dissertation for the Degree of Master). South China University of Technology, China.
- Zhang, Z. C., Su, G. H., Luo, C. L., Pang, Y. L., Wang, L., Li, X., Wen, J. H., & Zhang, J. L. (2015). Effects of anthocyanins from purple sweet potato (*Ipomoea batatas* L. cultivar Eshu No. 8) on the serum uric acid level and xanthine oxidase activity in hyperuricemic mice. *Food & Function*, 6(9), 3045-3055. <http://dx.doi.org/10.1039/C5FO00499C>. PMID:26201407.
- Zhang, Z. C., Wang, H. B., Zhou, Q., Hu, B., Wen, J. H., & Zhang, J. L. (2017). Screening of effective xanthine oxidase inhibitors in dietary anthocyanins from purple sweet potato (*Ipomoea batatas* L. Cultivar Eshu No.8) and deciphering of the underlying mechanisms in vitro. *Journal of Functional Foods*, 36, 102-111. <http://dx.doi.org/10.1016/j.jff.2017.06.048>.
- Zhong, H., Abdullah, Zhang, Y., Deng, L., Zhao, M., Tang, J., Zhang, H., Feng, F., & Wang, J. (2021). Exploring the potential of novel xanthine oxidase inhibitory peptide (ACECD) derived from Skipjack tuna hydrolysates using affinity-ultrafiltration coupled with HPLC-MALDI-TOF/TOF-MS. *Food Chemistry*, 347, 129068. <http://dx.doi.org/10.1016/j.foodchem.2021.129068>. PMID:33486365.
- Zhouhuang, S. (2018). *Study on uric acid-reducing peptide of tilapia skin collagen*. (Dissertation for the Degree of Master). South China University of Technology, China.